L.O. Copy — Mr R.J. Templin

L.O. NAE 638	**NATIONAL AERONAUTICAL ESTABLISHMENT**	NO. AE-46(p) HSAL-M-116
FILE BM2-17-14A-31	OTTAWA, CANADA	PAGE 1 OF
PREPARED BY LTC	**LABORATORY MEMORANDUM**	COPY NO. 4
CHECKED BY KOR	SECTION High Speed Aerodynamics	DATE 11 Sept., 1958

SECURITY CLASSIFICATION ~~Secret~~

SUBJECT Tests on .04 Scale Arrow Fin Model with I.R. Seeker Pod at Supersonic Speeds

PREPARED BY L.T. Conlin

ISSUED TO
Dr. D.C. MacPhail
Mr. J.H. Parkin
Mr. R.J. Templin (2)
Mr. K. Orlik-Rückemann (2)
Author
Aero Library (2)

LIST OF SYMBOLS

The results are presented with reference to axes parallel to the body axes, as illustrated in figure 3. Coefficients and symbols are defined as follows:-

C_{Y_v} side force coefficient of vertical tail, $\frac{Y}{qS_v}$

C_{B_v} root bending moment coefficient of vertical tail about the theoretical tail root (1.28 inch above the fuselage reference line), $\frac{B_v}{qS_v b_v}$

C_{n_v} yawing moment coefficient of vertical tail about a vertical axis through the 25 per cent point of the vertical tail mean geometric chord, $\frac{n_v}{qS_v \bar{c}_v}$

C_{h_r} rudder hinge moment coefficient, $\frac{H_r}{qS_r \bar{c}_r}$

a_1 rate of change of side force coefficient with angle of yaw, ψ $(\psi = -\beta)$

a_2 rate of change of side force coefficient with rudder angle, δ_r

q free stream dynamic pressure

S_v vertical tail area (from the theoretical root chord), 36.586 square inches.

S_r rudder area (aft of hinge line), 8.949 square inches

$\bar{c}_v$ mean geometric chord of vertical tail, 6.497 inches

$\bar{c}_r$ rudder r m s chord, 1.911 inch

b_v span of vertical tail (from the theoretical root) 6.180 inches

β angle of sideslip, degrees

δ_r rudder deflection angle, degrees, measured perpendicular to hinge line

$x_{a.c.}$ distance of the aerodynamic centre from the leading edge of $\bar{c}_v$

$x_{c.p.}$ distance of the centre of pressure from the leading edge of $\bar{c}_v$, due to rudder deflection

$z_{c.p.}$ distance of the centre of pressure from the vertical tail root chord, due to rudder deflection

p static pressure

p_o tunnel stagnation pressure

p_{o_1} total pressure

LIST OF FIGURES

INTRODUCTION

Tests have been made in the NAE 30" x 16" high speed wind tunnel on a .04 scale model of the vertical tail of the Avro Arrow aircraft to determine the effect of the I.R. seeker pod on the vertical tail characteristics and on rudder hinge moments.

The tests were made at Mach numbers 1.35, 1.78 and 2.03. The corresponding Reynolds number range was between 2.36 and 1.98 x 10^6.

MODEL

The 0.4 scale model of the vertical tail was mounted on a circular adapter plate which was fitted on the wall of the tunnel in such a manner that the model and plate could be rotated and clamped at the angle corresponding to the desired value of the angle of sideslip, β.

A three component strain gauge balance (side force, root bending moment and yawing moment) was installed on the model. The rudders were interchangeable (one for each rudder angle) and each was equipped with a strain gauge bridge to measure rudder hinge moment.

Interchangeable total pressure and static pressure probes were installed on the fin leading edge at .85 and .92 of the vertical tail height for pressure measurements.

A photograph of the model is shown in figure 1, and a drawing showing the I.R. seeker pod installed is presented in figure 2.

TEST TECHNIQUE

The three component balance consisted of three strain gauge bridges located on the cantilever beam which supported the model. Two of the bridges were sensitive to moments about a yaw axis and the third to moments about a roll axis. Since the centres of resolution of the yaw bridges were some distance apart, yawing moment and normal force could be obtained from their outputs. From the output of the third bridge the bending moment about the fin root chord could be obtained.

Rudder hinge moment was measured by means of a strain gauge bridge located on the attachment lug of each of the interchangeable rudders.

The test programme including pressure measurements is summarized in Table I.

Storage batteries provided the supply voltage for all strain gauge bridges. Outputs from the bridges were recorded on self-balancing potentiometer recorders.

A static calibration of the three component balance and of each of the rudder hinge moment bridges used in the tests was made prior to the tests. Calibration factors checked closely with those obtained in the previous calibration (reference 1).

A mercury manometer was used for measuring the static and total pressures.

DATA REDUCTION

Measured quantities were as follows:

M_1 forward moment (yawing moment about the centre of resolution of the forward moment bridge).

M_2 aft moment (yawing moment about the centre of resolution of the aft moment bridge).

M_3 root bending moment (rolling moment about the centre of resolution of the root bending moment bridge).

M_4 rudder hinge moment (about the rudder hinge line).

Side force, $Y = -\left(\frac{M_1 - M_2}{l}\right)$, where l is the distance between the centres of resolution of the forward and aft moment bridges. It follows that

$$C_Y = \frac{Y}{q S_v}$$

Yawing moment about the 25% point of the mean chord was obtained from the relation

$$M_{c/4} = M_1 + Yd$$

where d is the distance from the centre of resolution of the forward moment bridge to the 25% point of the mean chord. In coefficient form

$$C_{n_v} = \frac{M_{c/4}}{q S_v \bar{c}_v}$$

Root bending moment (about fin root chord) was obtained from M_3

$$B_v = M_3 - Yh$$

where h is the distance from the centre of resolution of the root bending moment bridge to the fin root chord. In coefficient form

$$C_{B_v} = \frac{B_v}{q S_v b_v}$$

Positions of aerodynamic centre and centre of pressure were derived as follows:

$$\frac{x_{a.c.}}{\bar{c}_v} = .25 - \left(\frac{\partial C_{n_v}}{\partial C_{Y_v}}\right)_{\delta_r = 0^\circ}$$

$$\frac{x_{c.p.}}{\bar{c}_v} = .25 - \frac{\left(\partial C_{n_v}/\partial \delta_r\right)_{\substack{\delta_r = 0^\circ \\ \beta = 0^\circ}}}{\left(\partial C_{Y_v}/\partial \delta_r\right)_{\substack{\delta_r = 0^\circ \\ \beta = 0^\circ}}}$$

$$\frac{z_{c.p.}}{b_v} = \frac{\left(\partial C_{B_v}/\partial \delta_r\right)_{\substack{\delta_r = 0^\circ \\ \beta = 0^\circ}}}{\left(\partial C_{Y_v}/\partial \delta_r\right)_{\substack{\delta_r = 0^\circ \\ \beta = 0^\circ}}}$$

Rudder hinge moment was obtained from M_4, $C_{h_r} = \frac{M_4}{q S_r \bar{c}_r}$.

The measured static pressures have been referred to stagnation pressure and the pressure ratio P/P_0 plotted against Mach number. The difference between the stagnation pressure and measured total pressure has been referred to q and the values of the ratio $\left(\frac{P_0 - P_{0_1}}{q}\right)$ have been plotted against Mach number.

CORRECTIONS AND ACCURACY

The measured values of δ_r with zero load were the same as in the previous tests on the model (reference 1) and were corrected for deflection under load; the nominal values of β were corrected for deflection also.

The estimated possible errors in derived quantities were as follows:

C_{Y_v}	±.006
C_{n_v}	±.003
C_{B_v}	±.0019
C_{h_r}	±.0015

RESULTS

The results of the force tests are presented in figures 5 to 16, and the results of the pressure measurements in Tables II and III and figures 17 to 19.

DISCUSSION OF RESULTS

The results of the tests made without the I.R. seeker pod installed agreed closely with the results of the same tests made previously (reference 1).

There was found to be no appreciable effect on the model fin characteristics due to the addition of the pod except at Mach number 2.03. Even at that Mach number the effect was not large but showed up mainly in the values of C_{Y_V} and C_{n_V} at the higher values of β. The shift in either aerodynamic centre or centre of pressure is small. It should be kept in mind when examining figures 15 and 16 that the experimental error in the determination of aerodynamic centre and centre of pressure at Mach number 1.78 is large due to the fact that the curve for C_{n_V} vs C_{Y_V} , was extrapolated, and that an insufficient number of points were available to accurately determine $\partial C_{n_V}/\partial \delta_N$, $\partial C_{Y_V}/\partial \delta_N$, and $\partial C_{B_V}/\partial \delta_N$.

The values of $\partial C_{\ell_V}/\partial \delta_N$ with the I.R. seeker pod added were found to be consistently less than for the case without the pod (reference 1).

REFERENCE

1. L.T. Conlin — Wind Tunnel Tests of 0.04 Scale Model of Avro C-105 Vertical Tail at Supersonic Speeds
Laboratory Memorandum NAE-503, October 1957.

TABLE I

SUMMARY OF TESTS

Mach Number			I.R. Pod	Pressure Measured
1.35	0	4	On	Total Pressure
	0	8	On	" "
	-5	0	On	Static Pressure
	-5	8	On	" "
	10	0	On	Total Pressure
	20	0	On	" "
	30	0	On	" "
	0	0	Off	Static Pressure
	0	8	Off	" "
	0	0	Off	Total Pressure
	0	4	Off	" "
	0	8	Off	" "
1.78	0	4	On	Total Pressure
	0	8	On	" "
	-5	0	On	Static Pressure
	-5	8	On	" "
	10	0	On	Total Pressure
	20	0	On	" "
2.03	0	-4	Off	Total Pressure
	0	0	Off	" "
	0	4	Off	" "
	0	8	Off	" "
	0	12	Off	" "
	-5	0	Off	" "
	-5	8	Off	" "
	0	-4	On	" "
	0	0	On	" "
	0	4	On	" "
	0	8	On	" "
	0	12	On	" "
	-5	-4	On	Static Pressure
	-5	0	On	" "
	-5	4	On	" "
	-5	8	On	" "
	-5	12	On	" "
	10	0	On	Total Pressure
	20	0	On	" "
	0	0	Off	Static Pressure
	0	8	Off	" "

TABLE II

STATIC PRESSURE MEASUREMENTS

Run	Mach No.	δ_r	β	Pod	P_o	P *Upper	P *Lower	P/P_o *Upper	P/P_o *Lower
13	1.35	0	0	Off	710.4	269.1	267.6	.379	.377
14	1.35	0	8	Off	710.4	249.6	260.5	.352	.367
27	1.35	-5	8	On	716.5	259.0	280.1	.362	.391
28	1.35	-5	0	On	716.2	266.2	265.4	.372	.371
32	1.35	-5	0	On	709.8	248.4	229.7	.350	.324
33	1.35	-5	8	On	708.8	234.0	247.4	.330	.349
34	1.78	-5	8	On	723.9	149.9	131.9	.207	.182
34R	1.78	-5	8	On	724.2	148.6	131.3	.205	.181
35	1.78	-5	0	On	724.4	503.1	143.2	.695	.198
11	2.03	0	8	Off	732.8	119.4	125.7	.163	.1717
12	2.03	0	0	Off	732.8	123.2	120.4	.168	.1647
20	2.03	-5	8	On	734.4	116.8	107.7	.1591	.1466
20R	2.03	-5	8	On	734.4	116.8	107.3	.1591	.1461
21	2.03	-5	12	On	737.2	127.9	102.7	.1736	.1394
22	2.03	-5	4	On	737.2	115.8	112.2	.1572	.1523
23	2.03	-5	0	On	737.2	114.3	112.1	.1551	.1522
24	2.03	-5	-4	On	737.2	114.5	111.6	.1554	.1515

*"Upper" and "Lower" refer to probe positions on the fin. Values of pressure are given in mm. mercury.

TABLE III

SUMMARY OF TOTAL PRESSURE MEASUREMENTS

Mach No.	δ_r	β	Pod	P_o	Total Press. (P_{o_1}) *Upper	*Lower	($P_o - P_{o_1}$) *Upper	*Lower	($P_o - P_{o_1}$)/q *Upper	*Lower	q
1.35	0	0	Off	715.1	691.5	688.6	23.6	26.5	.0768	.0862	307.4
1.35	0	8	Off	715.7	692.3	691.8	23.4	23.9	.0762	.0778	307.6
1.35	0	4	Off	715.8	692.7	690.5	23.1	25.3	.0751	.0822	307.8
1.35	0	4	On	715.8	691.7	682.5	24.1	33.3	.0783	.1081	307.8
1.35	0	8	On	715.7	691.8	681.0	23.9	34.7	.0778	.1128	307.6
1.35	10	0	On	715.8	691.3	682.8	24.5	33.0	.0796	.1072	307.8
1.35	30	0	On	715.6	691.6	682.7	24.0	32.9	.0780	.1068	307.8
1.35	20	0	On	709.5	695.1	684.0	14.4	25.5	.0472	.0836	305.0
1.78	0	4	On	724.6	599.7	598.1	124.9	126.5	.4335	.439	288.1
1.78	0	8	On	724.9	603.1	610.3	121.8	114.6	.4225	.3975	288.3
1.78	10	0	On	725.6	595.9	589.8	129.7	135.8	.450	.471	288.5
1.78	20	0	On	725.8	596.3	590.4	129.5	135.4	.449	.469	288.7
2.03	0	0	Off	735.3	597.8	586.2	155.5	149.1	.6015	.576	258.8
2.03	0	4	Off	735.2	584.0	589.3	151.2	145.9	.585	.564	258.8
2.03	0	8	Off	735.1	598.2	599.4	136.9	135.7	.529	.525	258.7
2.03	0	12	Off	734.8	610.2	612.2	124.6	122.6	.482	.475	258.5
2.03	0	-4	Off	734.8	578.2	580.5	156.6	154.3	.606	.597	258.5
2.03	0	-4	On	733.8	548.5	539.8	185.3	194.0	.718	.7515	258.2
2.03	0	0	On	733.8	540.8	532.7	193.0	201.1	.748	.779	258.2
2.03	0	4	On	733.8	547.7	542.2	186.1	191.6	.721	.742	258.2
2.03	0	8	On	733.8	555.4	553.2	178.4	180.6	.691	.700	258.2
2.03	0	12	On	733.8	559.0	549.5	174.8	184.3	.677	.714	258.2
2.03	-5	0	Off	737.1	566.6	575.3	170.5	161.8	.658	.624	259.2
2.03	-5	8	Off	737.1	597.5	600.0	139.6	137.1	.539	.529	259.2
2.03	20	0	On	732.4	547.1	541.4	185.3	191	.720	.742	257.6
2.03	10	0	On	732.8	548.0	542.3	184.8	190.5	.718	.739	257.8

*"Upper" and "Lower" refer to probe positions on the fin.
Values of pressure and of q are given in mm. mercury.

Fig. 1 The .04 Scale Arrow (C-105) Vertical Tail

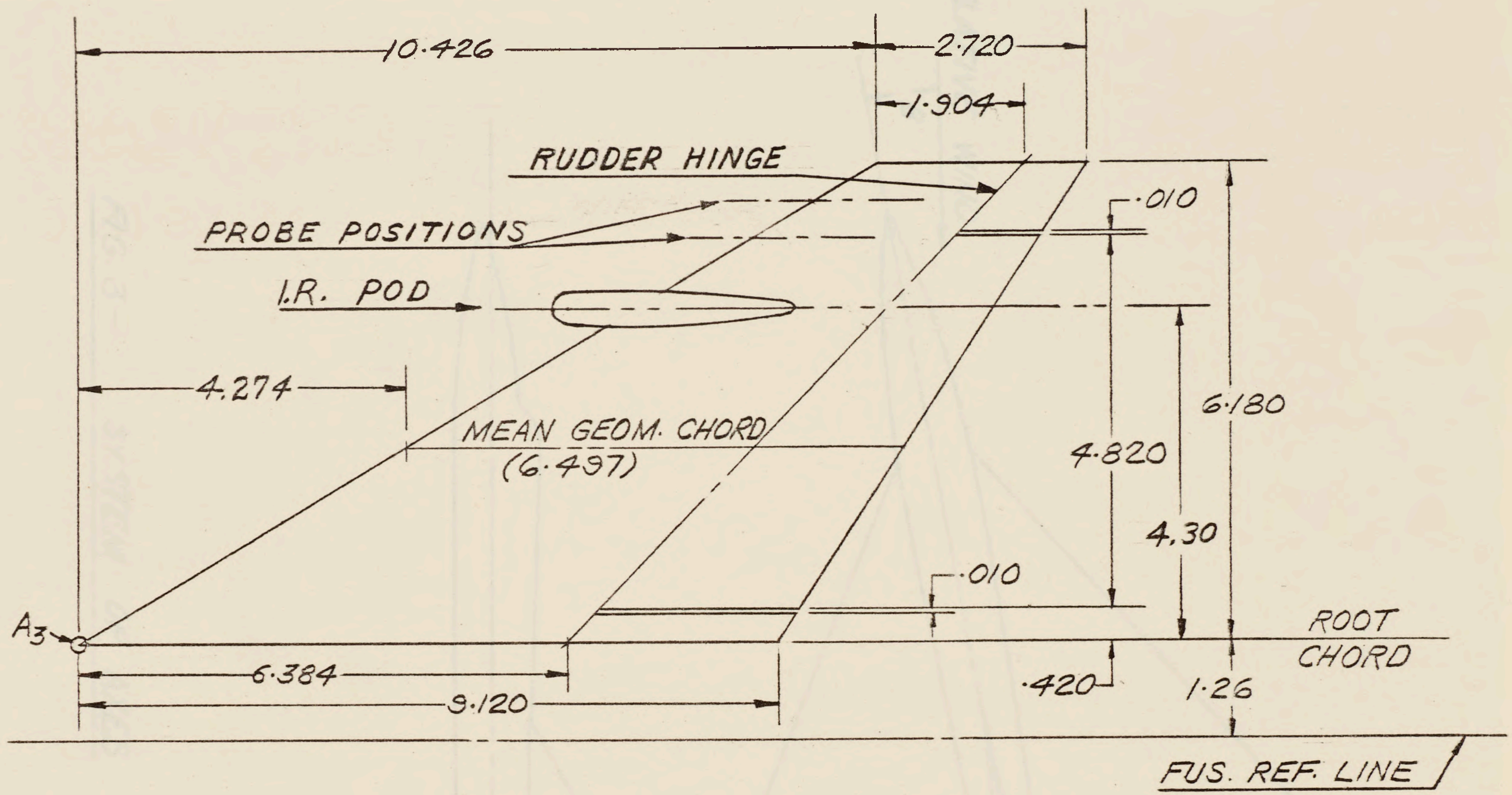

FIG. 2— C-105 VERTICAL TAIL, ·04 SCALE

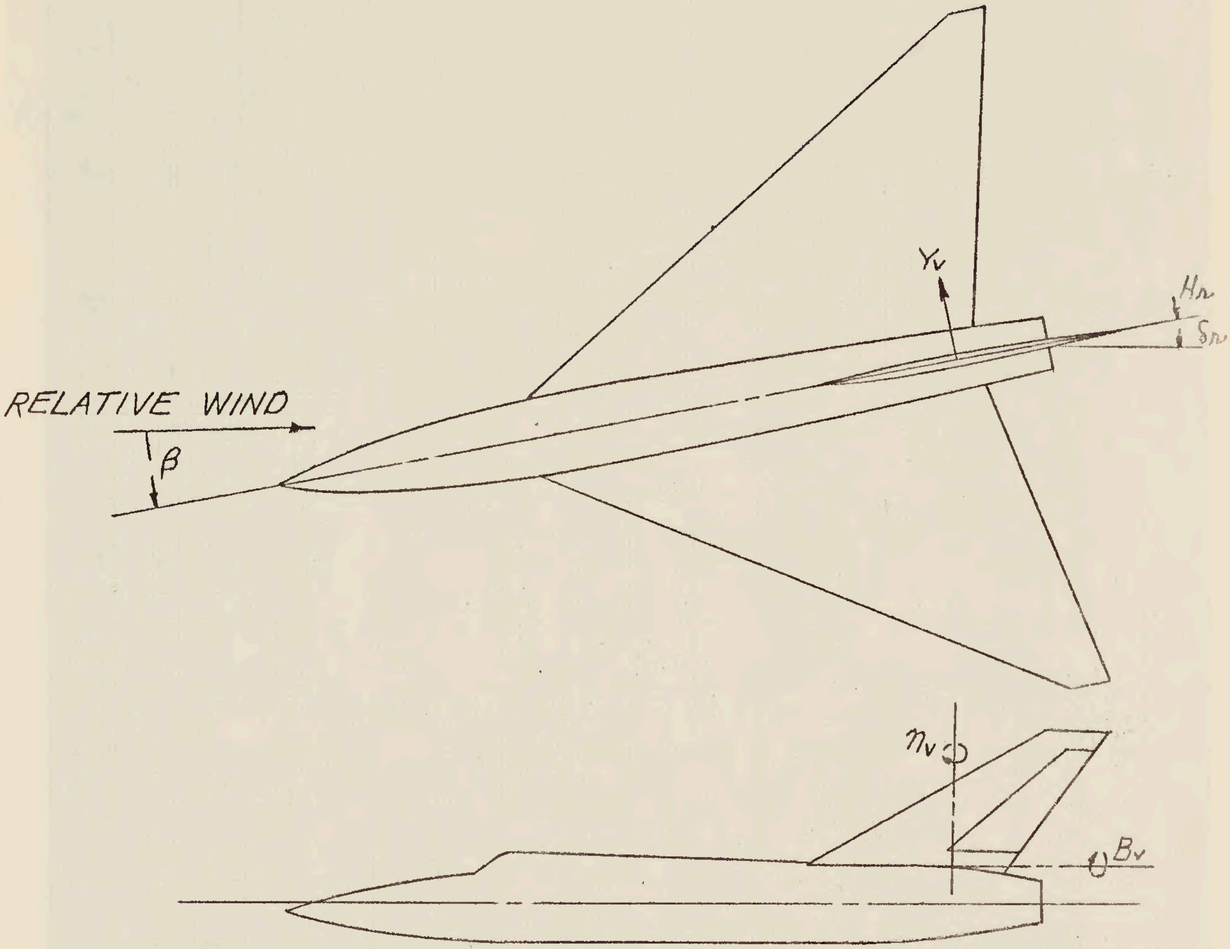

FIG. 3 — SYSTEM OF AXES

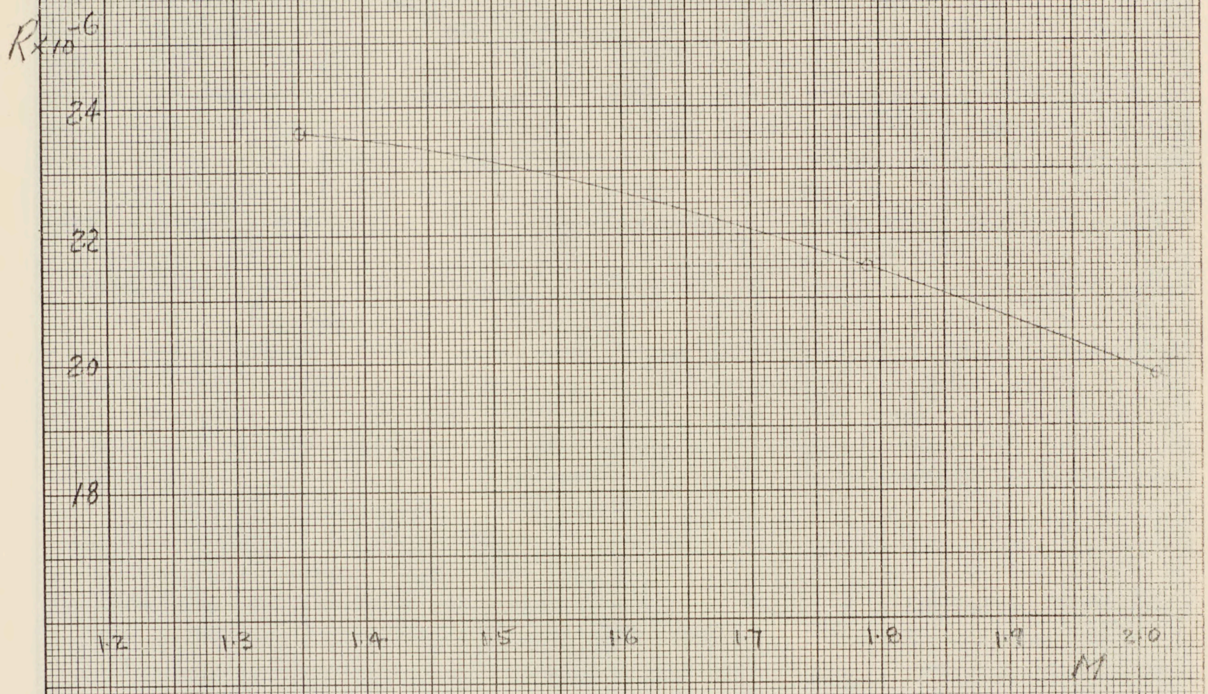

FIG. 4 MODEL REYNOLDS NUMBER (BASED ON FIN MEAN GEOMETRIC CHORD) VS. MACH NUMBER

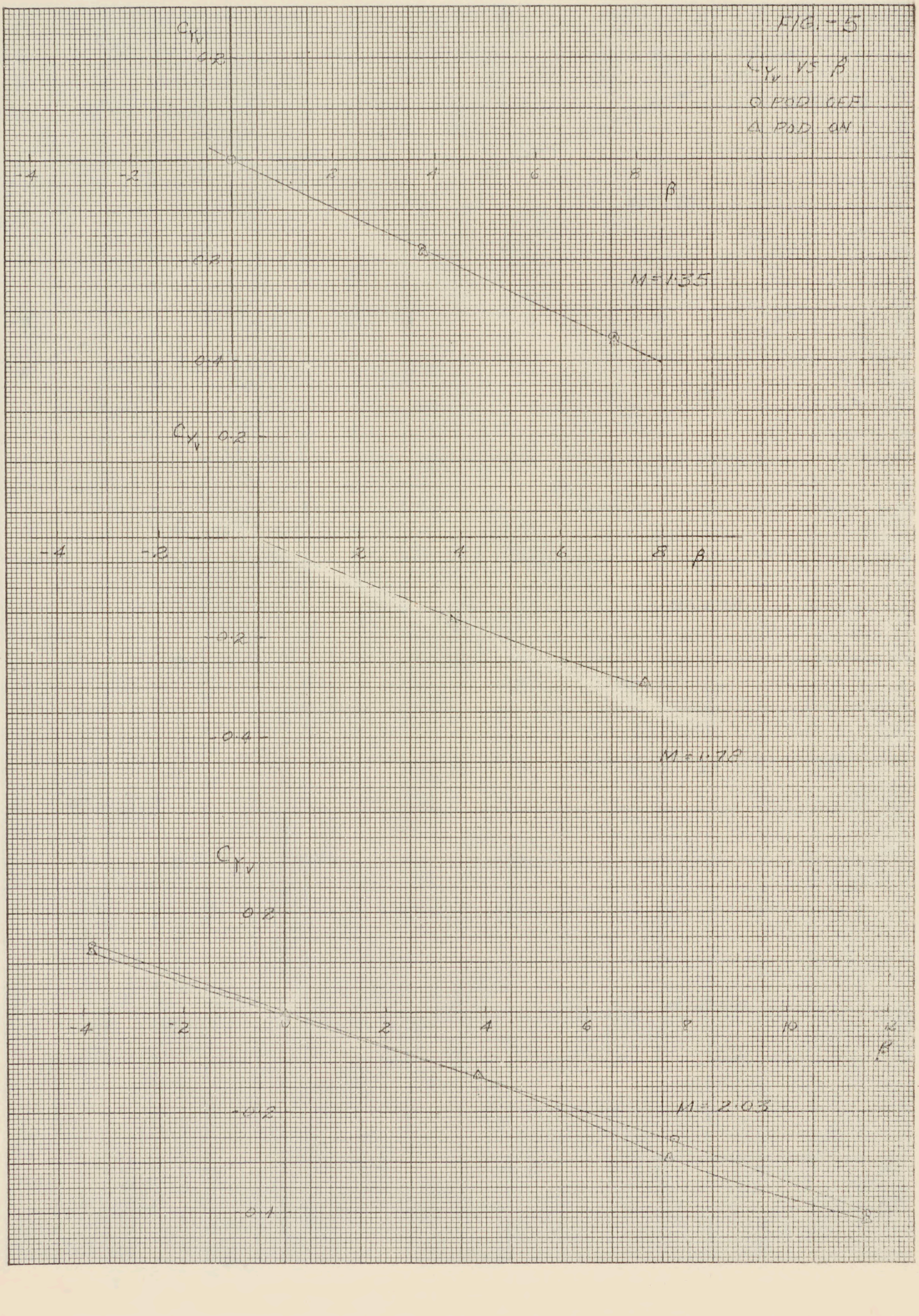
FIG. 5
C_{Y_v} VS β
○ POD OFF
△ POD ON
M = 1.35
M = 1.78
M = 2.03
C_{Y_v}
β

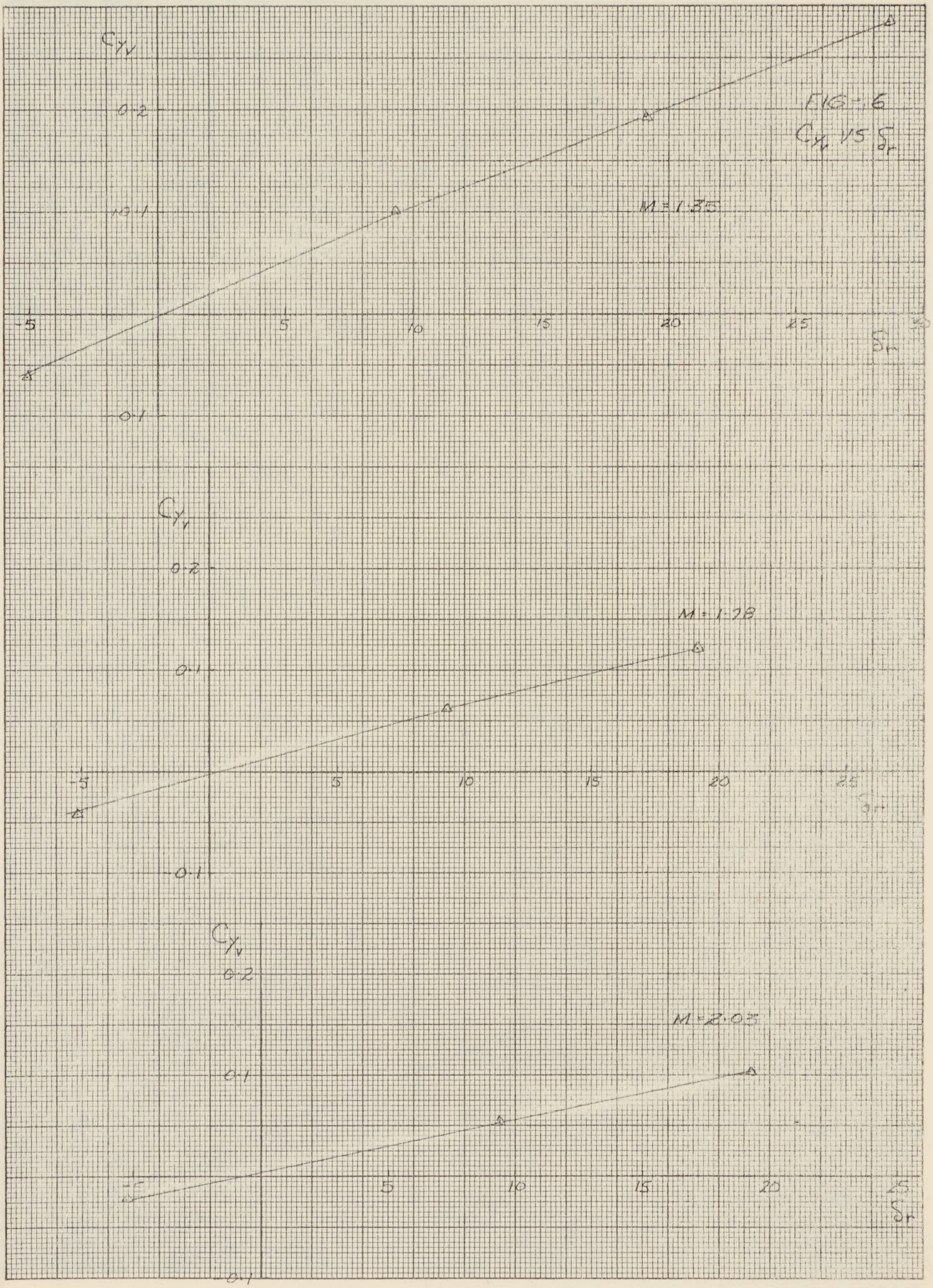
FIG. 6
C_{Y_v} VS δ_r
M = 1.35
M = 1.78
M = 2.03
C_{Y_v}
δ_r
0.2
0.1
-0.1
-5
5
10
15
20
25

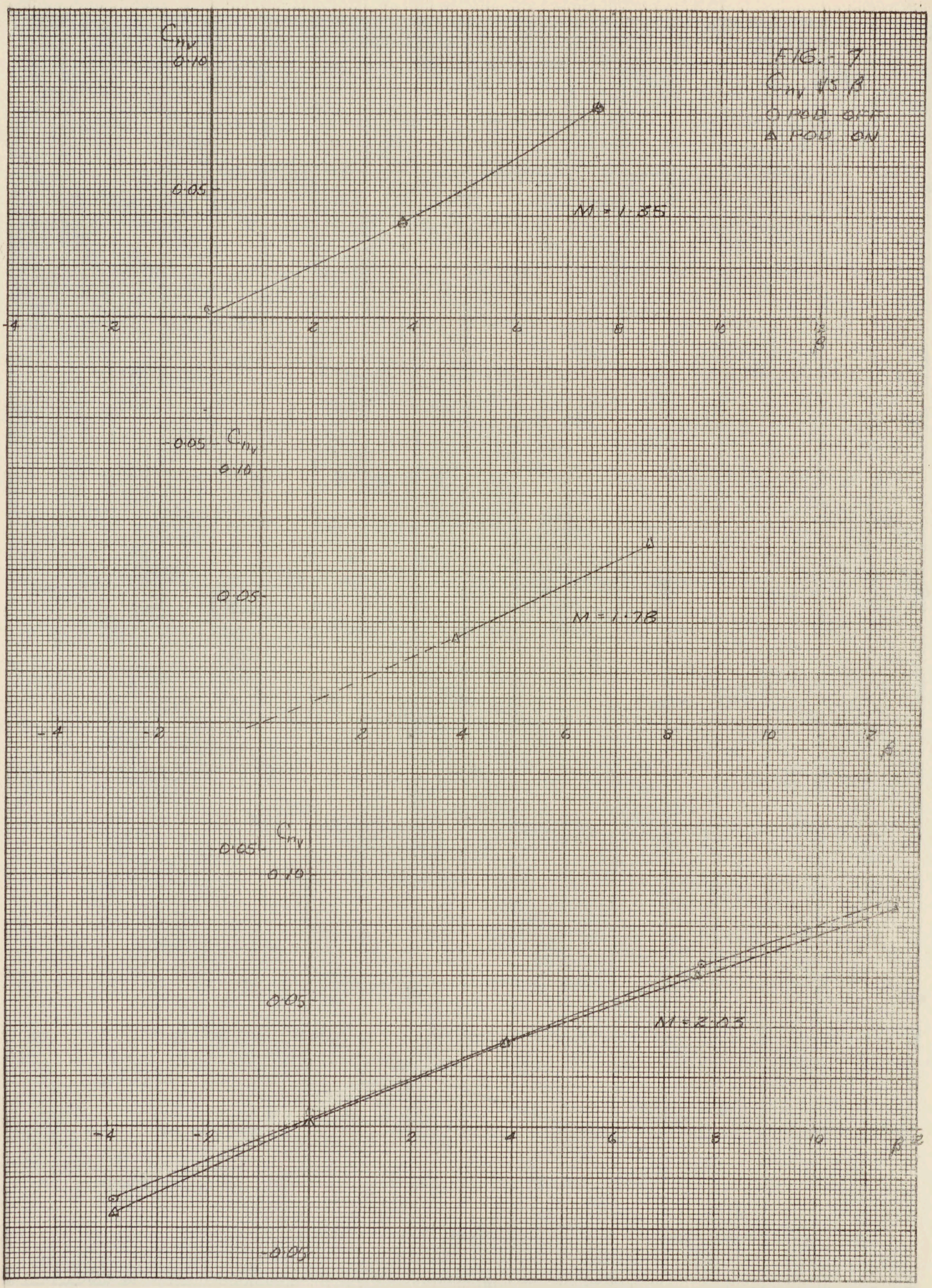
FIG. - 7
C_{n_V} VS β
○ POD OFF
△ POD ON
C_{n_V}
0.10
0.05
-0.05
M = 1.35
M = 1.78
M = 2.03
-4
-2
2
4
6
8
10
12
β

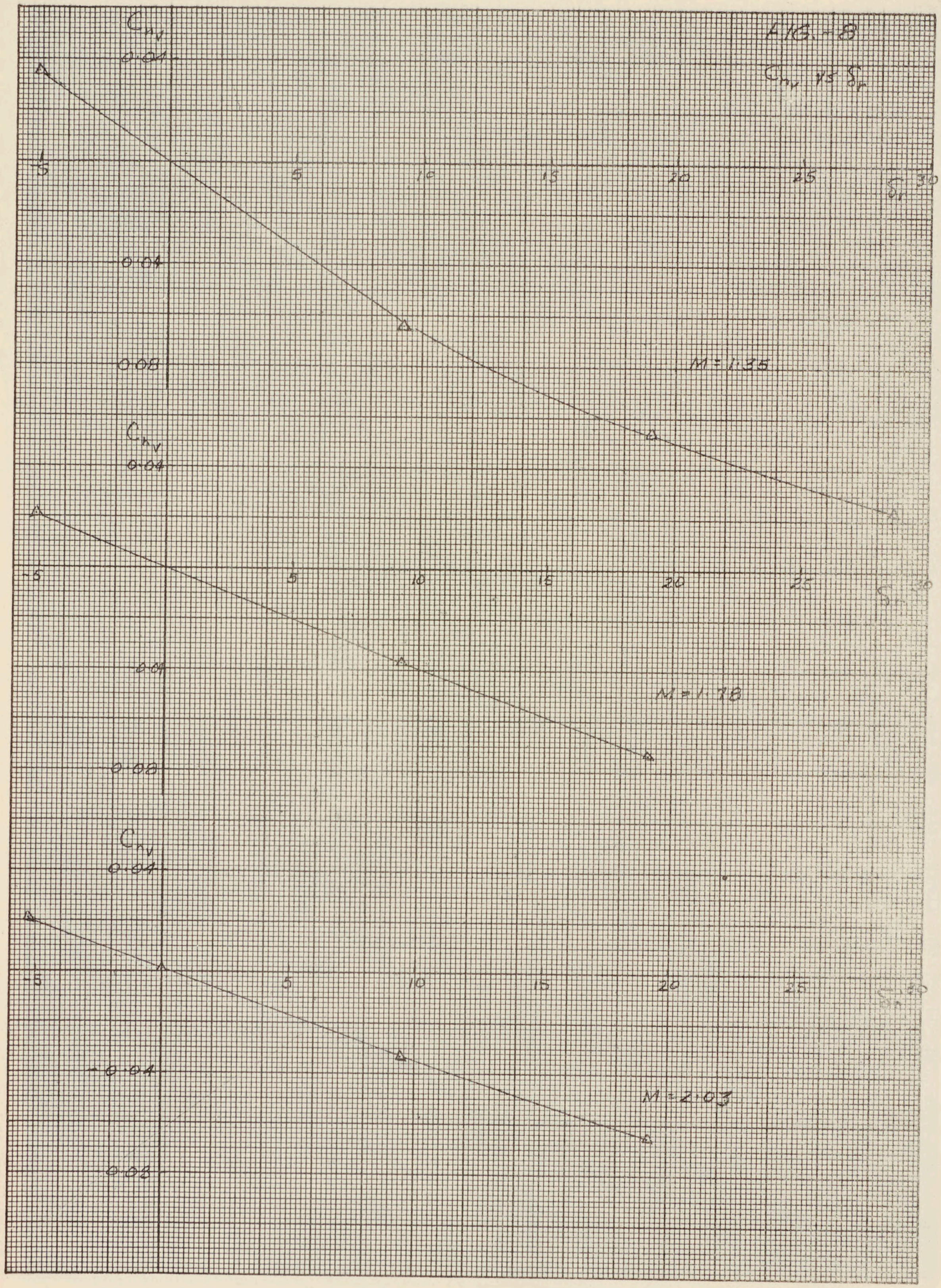
FIG. 8
C_{n_v} vs δ_r
C_{n_v}
0.04
-5
5
10
15
20
25
30
δ_r
0.04
0.08
M = 1.35
C_{n_v}
0.04
-5
5
10
15
20
25
30
δ_r
0.04
0.08
M = 1.78
C_{n_v}
0.04
-5
5
10
15
20
25
30
δ_r
-0.04
0.08
M = 2.03

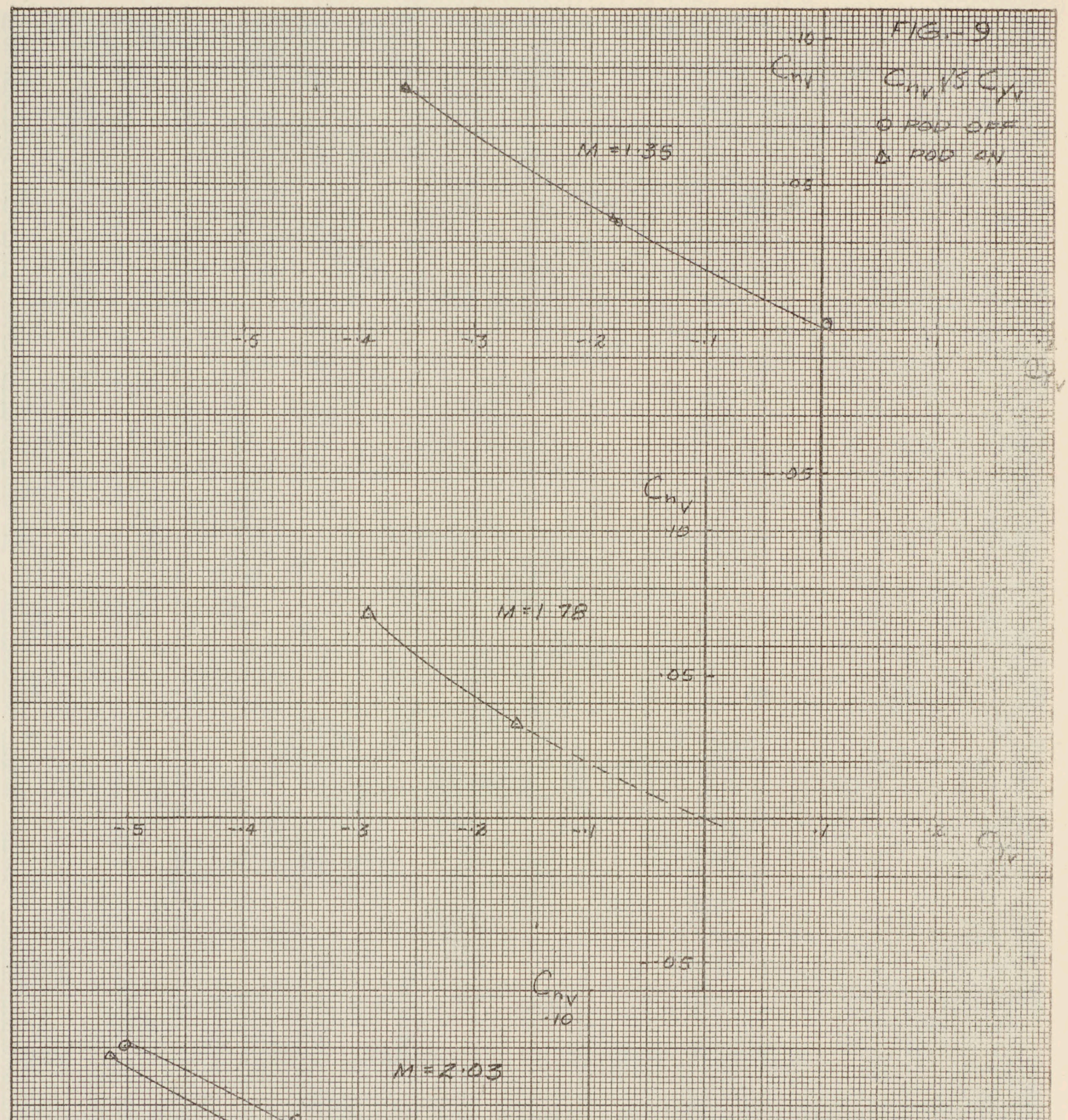
FIG. 9
C_{n_V} VS C_{Y_V}
○ POD OFF
△ POD ON
M = 1·35
M = 1·78
M = 2·03
C_{n_V}
C_{Y_V}

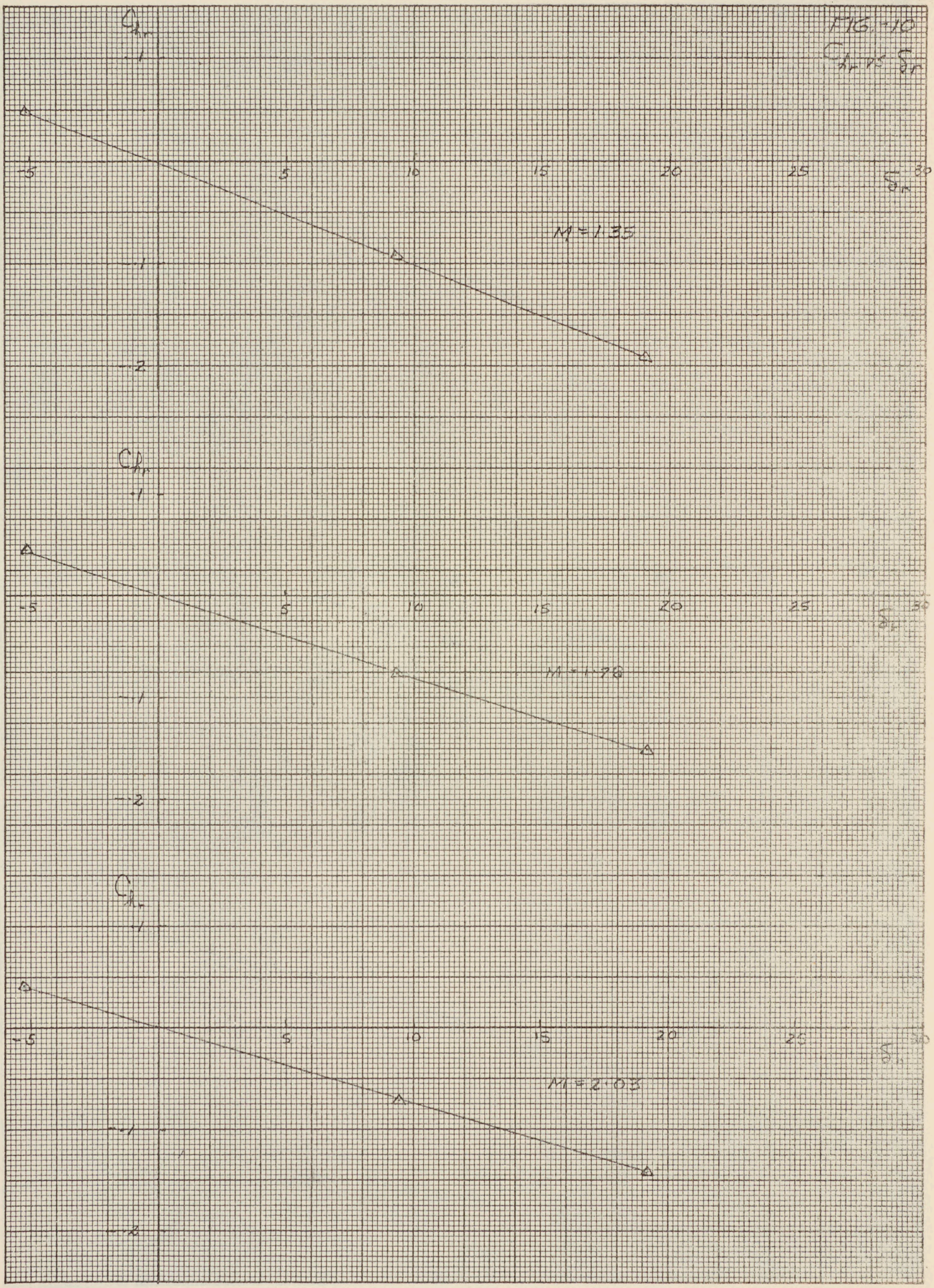

FIG. 10
C_{h_r} vs δ_r
C_{h_r}
M = 1.35
M = 1.76
M = 2.03
δ_r

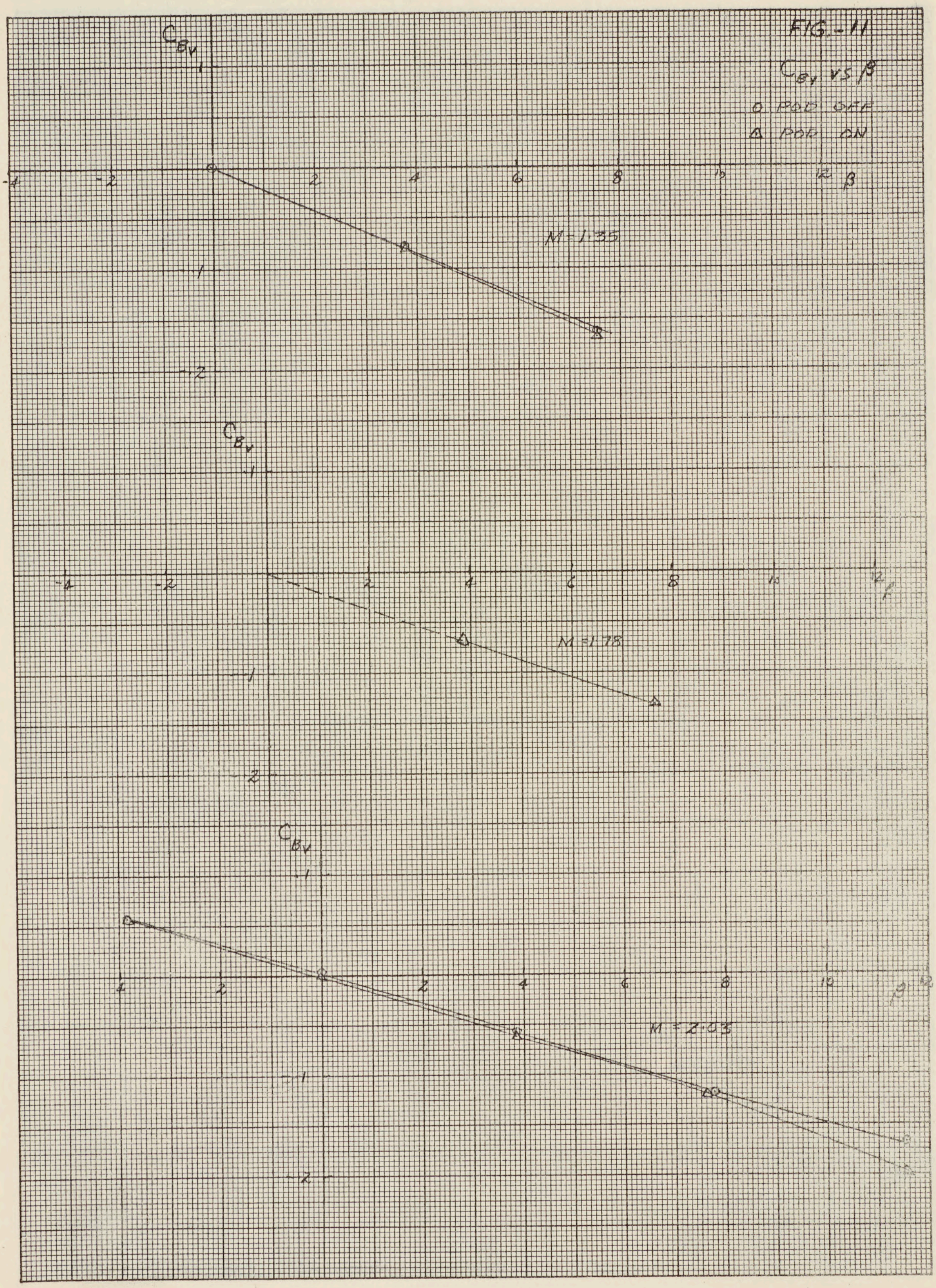

FIG - 11
C_{BV} vs β
○ POD OFF
△ POD ON
M = 1.35
M = 1.78
M = 2.03
C_{BV}
β

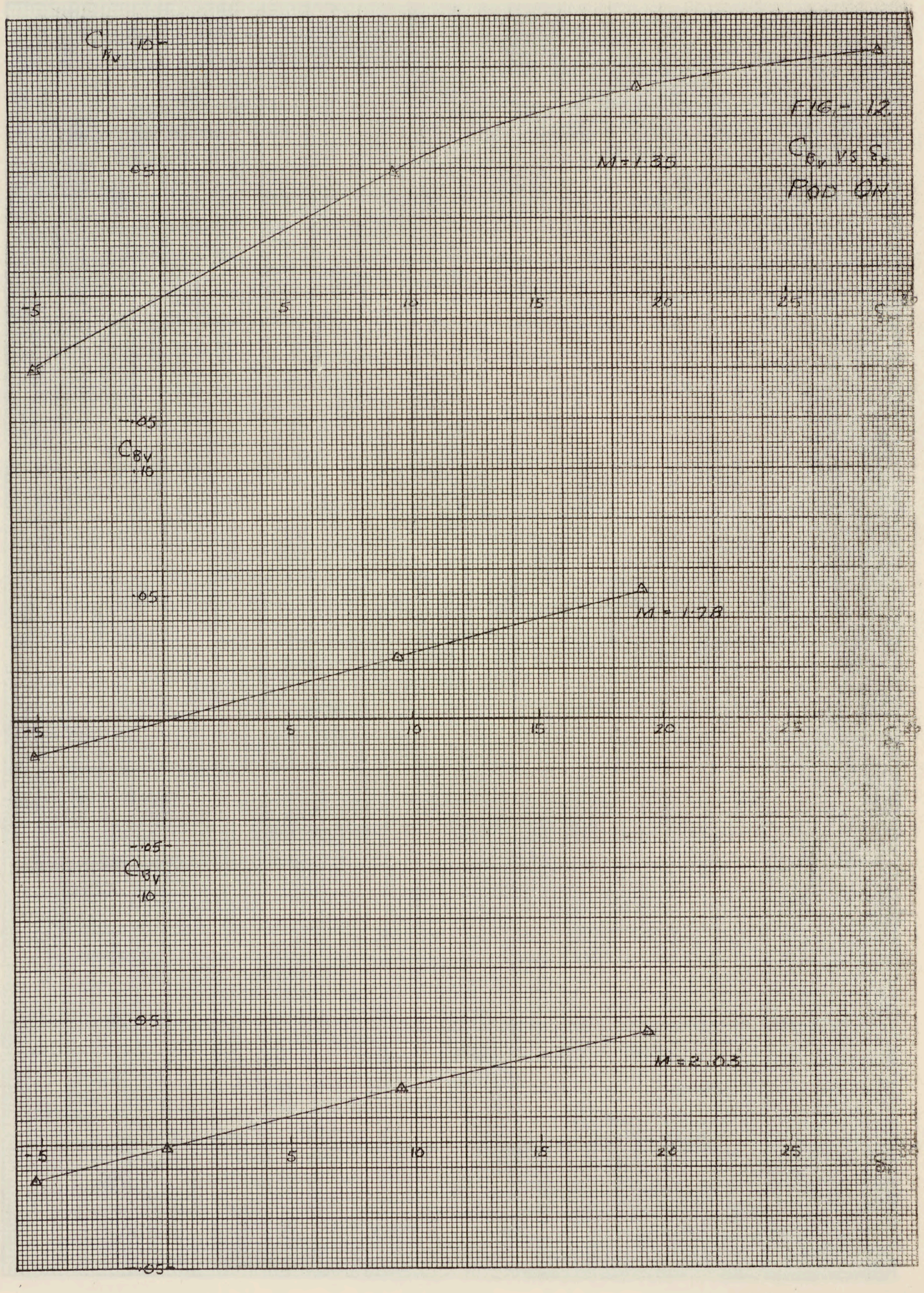
FIG - 12
C_{B_V} VS δ_t
POD QH
M = 1.35
M = 1.78
M = 2.03
C_{B_V}
.10
.05
-.05
-5
5
10
15
20
25
δ_t

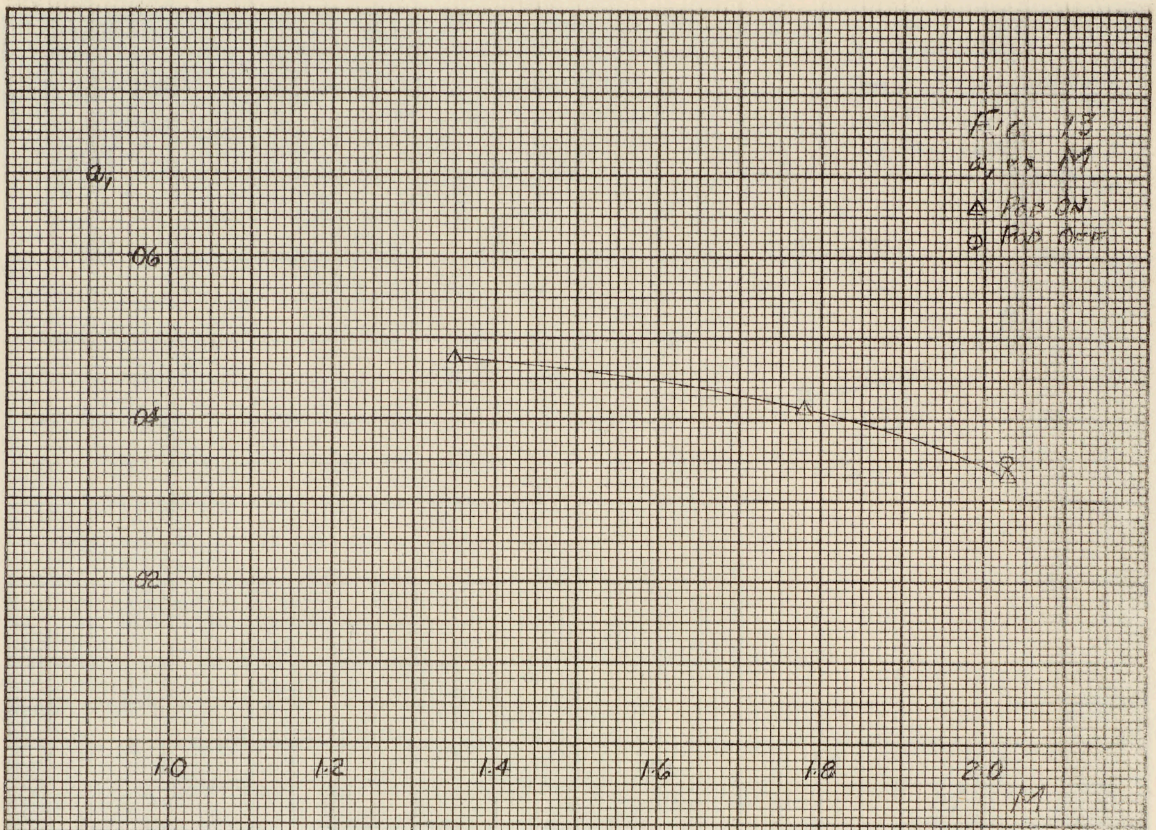
FIG 13
a₁ vs M
△ Rod ON
○ Rod OFF
a₁
.06
.04
.02
1.0
1.2
1.4
1.6
1.8
2.0
M

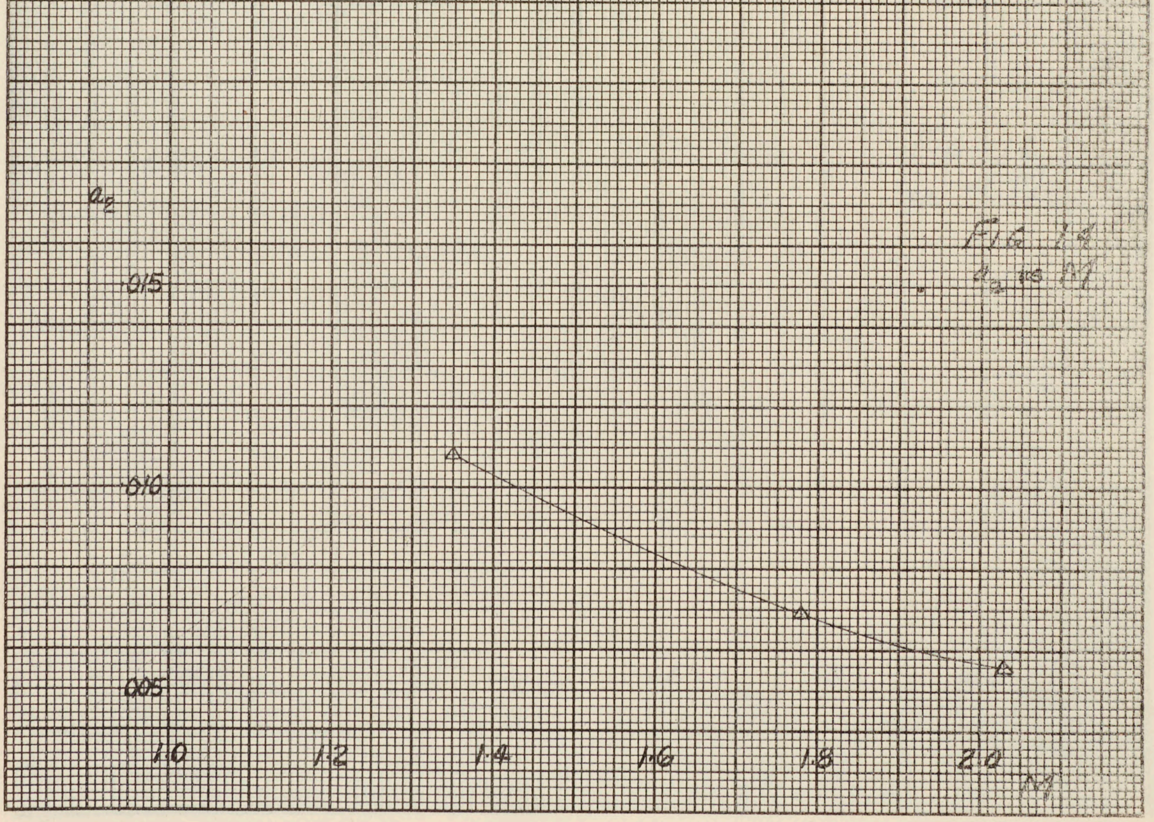
FIG 14
a₂ vs M
a₂
.015
.010
.005
1.0
1.2
1.4
1.6
1.8
2.0
M

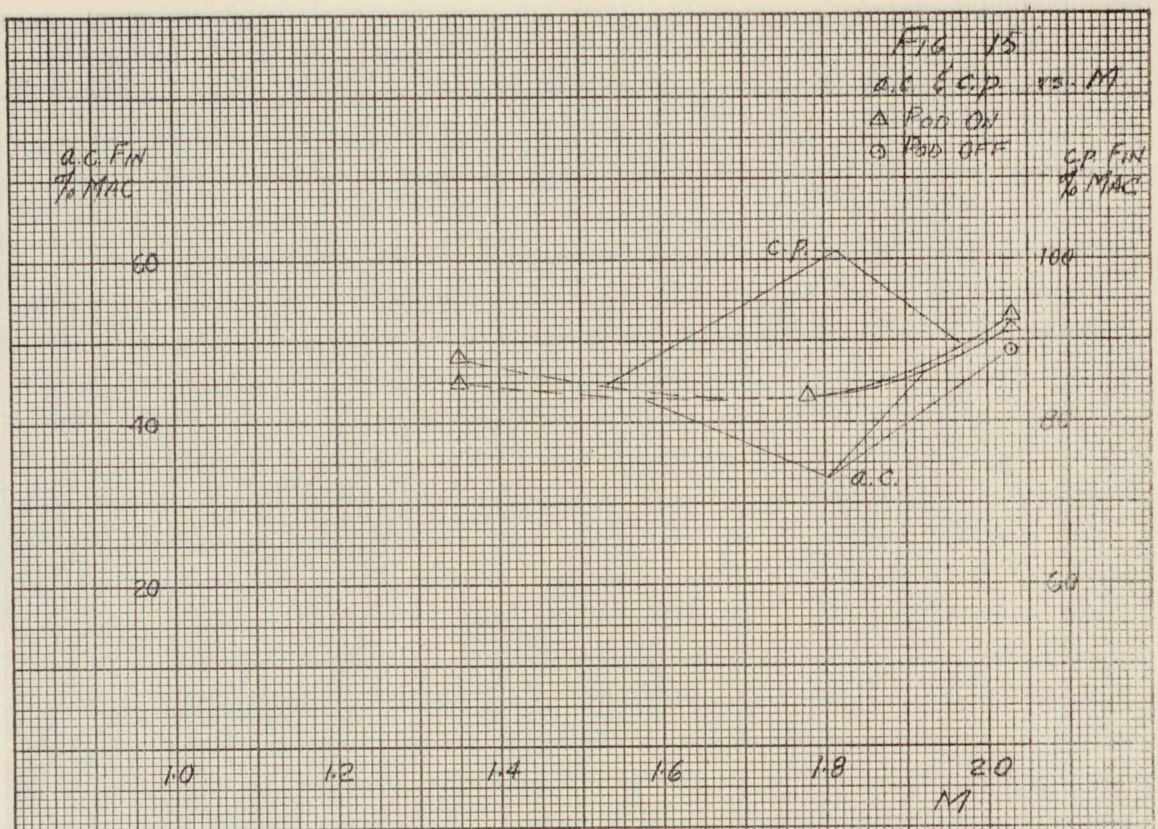
FIG 15
a.c. & c.p. vs. M
△ POD ON
⊙ POD OFF
a.c. FIN % MAC
c.p. FIN % MAC
c.p.
a.c.
60
40
20
100
80
60
1.0
1.2
1.4
1.6
1.8
2.0
M

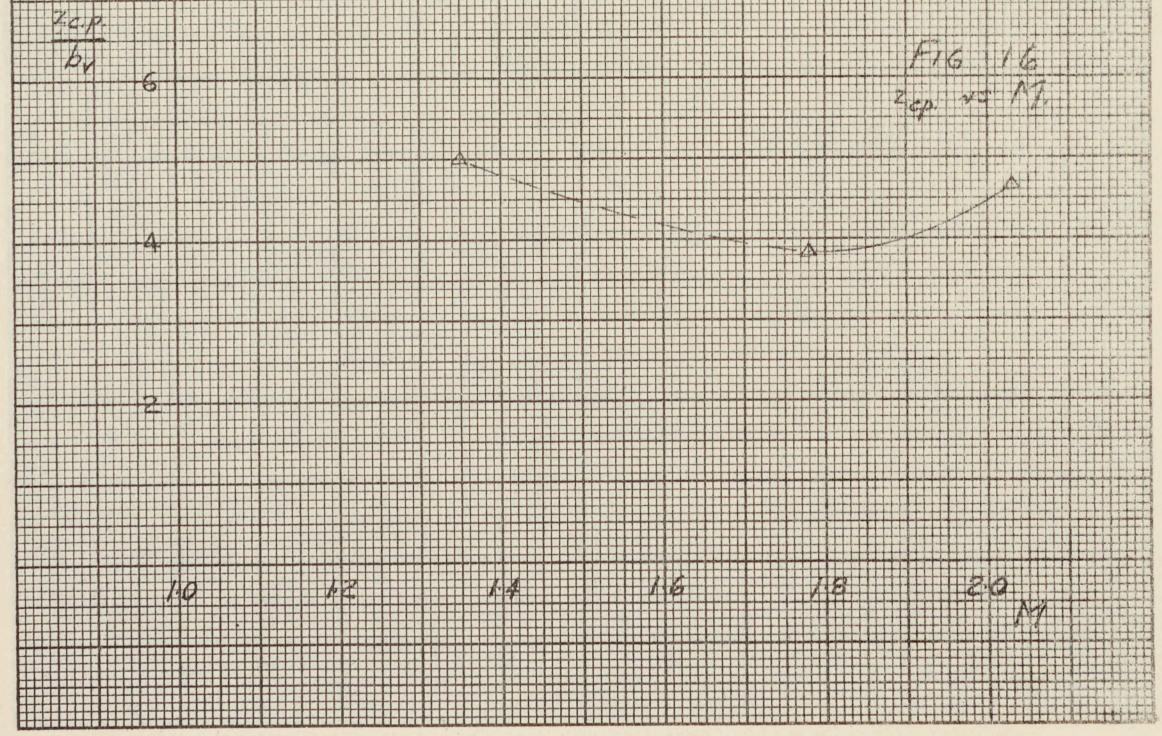
FIG 16
z_{cp} vs M
$\frac{z_{c.p.}}{b_v}$
6
4
2
1.0
1.2
1.4
1.6
1.8
2.0
M

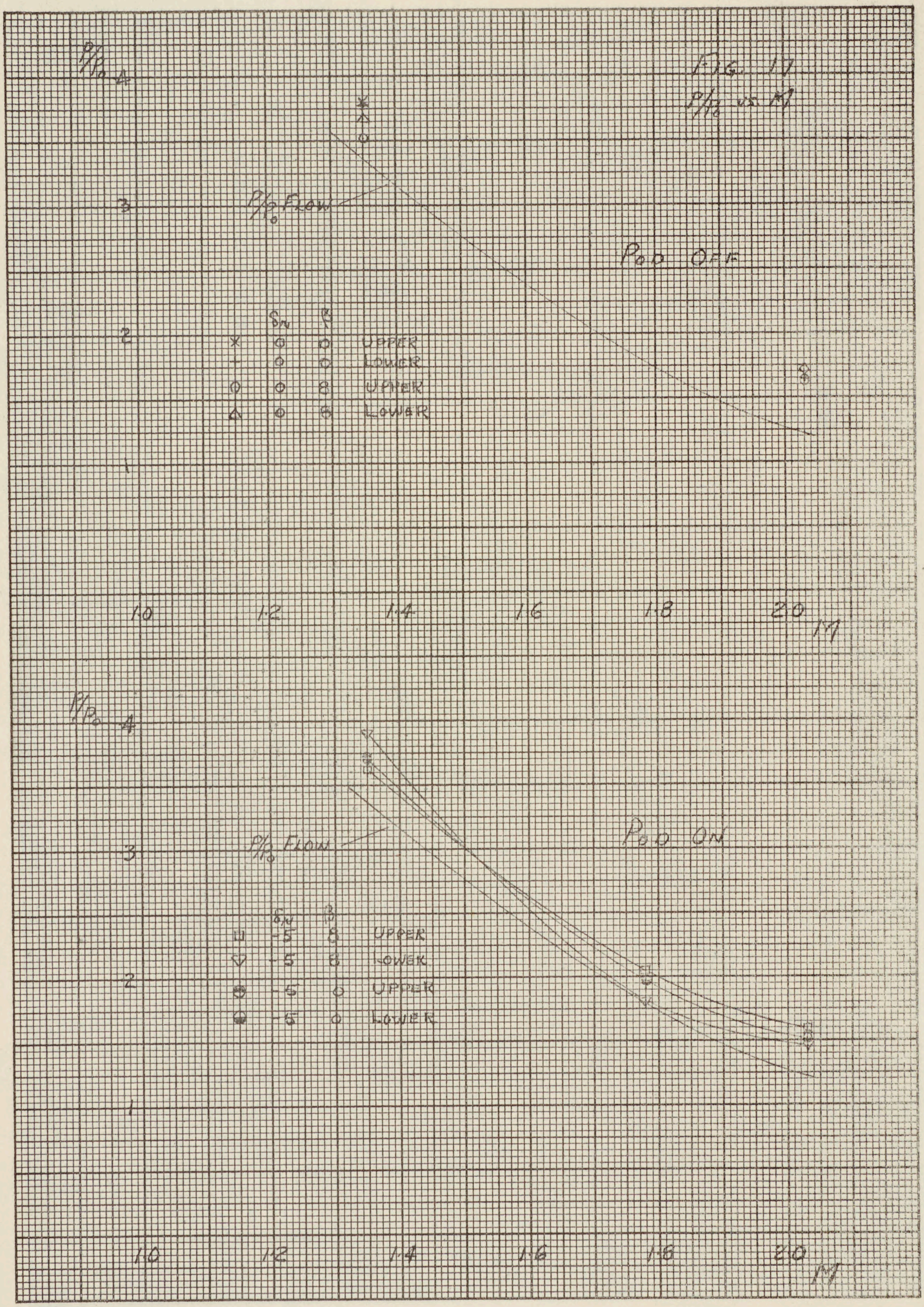

FIG. 17
P/P0 vs M
P/P0
4
3
2
1
P/P0 FLOW
POD OFF
δN δ
× 0 0 UPPER
+ 0 0 LOWER
○ 0 8 UPPER
△ 0 8 LOWER
1.0 1.2 1.4 1.6 1.8 2.0 M
P/P0
4
3
2
1
P/P0 FLOW
POD ON
δN δ
□ -5 8 UPPER
▽ -5 8 LOWER
⊕ -5 0 UPPER
● -5 0 LOWER
1.0 1.2 1.4 1.6 1.8 2.0 M

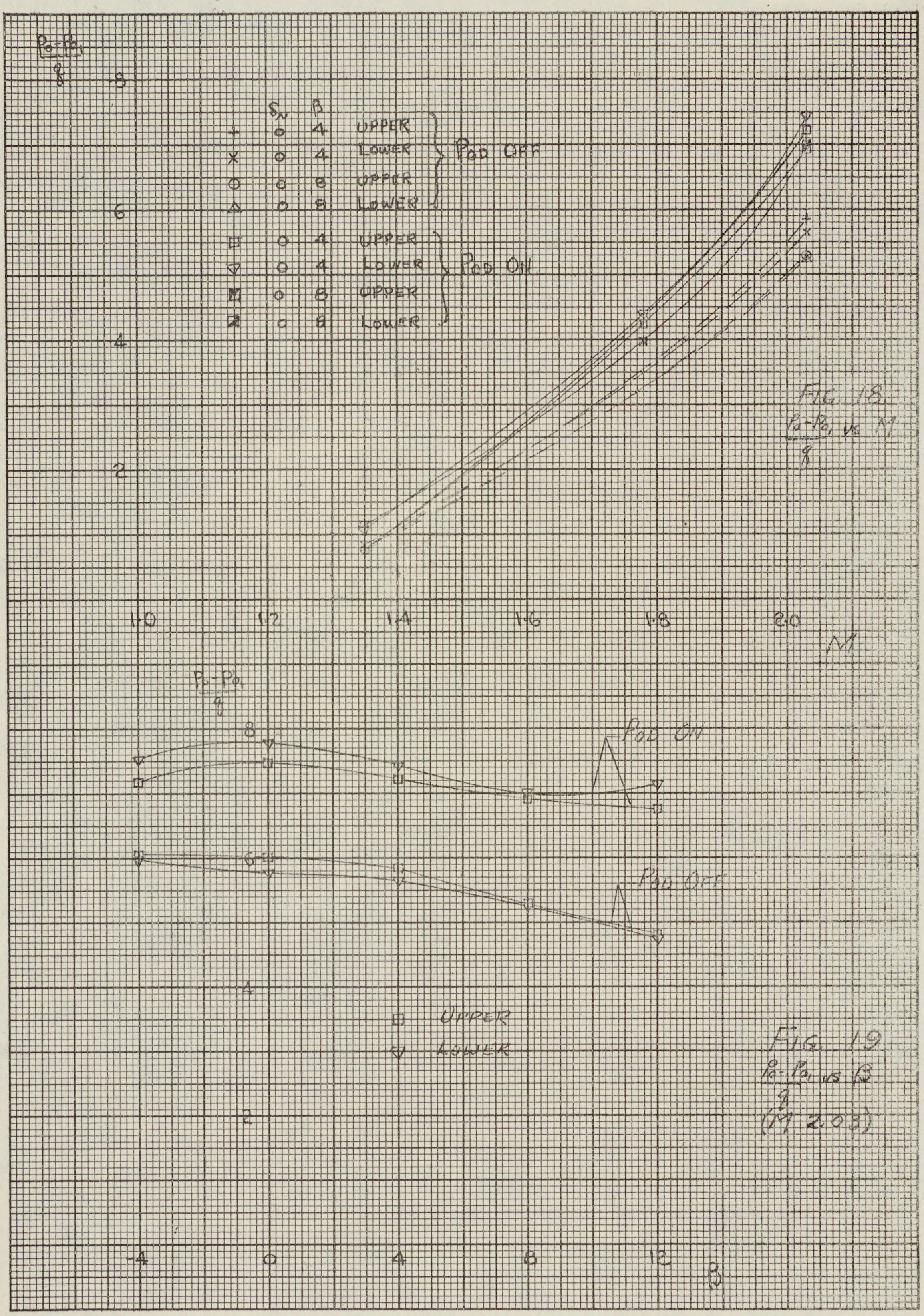

Po-P∞ / q
8
6
4
2
Sv β
+ 0 4 UPPER
× 0 4 LOWER
⊙ 0 8 UPPER
△ 0 8 LOWER
POD OFF
⊞ 0 4 UPPER
▽ 0 4 LOWER
⊠ 0 8 UPPER
⊿ 0 8 LOWER
POD ON
1.0
1.2
1.4
1.6
1.8
2.0
M
FIG. 18
Po-P∞ / q vs M
Po-P∞ / q
8
6
4
2
POD ON
POD OFF
□ UPPER
▽ LOWER
-4
0
4
8
12
β
FIG. 19
Po-P∞ / q vs β
(M 2.03)